2014

Resting-state modulation of alpha rhythms by interference with angular gyrus activity

Paolo Capotosto
Gabriele d'Annunzio University

Claudio Babiloni
University of Rome La Sapienza

Gian Luca Romani
Gabriele d'Annunzio University

Maurizio Corbetta
Washington University School of Medicine in St. Louis

Resting-state Modulation of Alpha Rhythms by Interference with Angular Gyrus Activity

Paolo Capotosto[1], Claudio Babiloni[2,3], Gian Luca Romani[1], and Maurizio Corbetta[1,4]

Abstract

■ The default mode network is active during restful wakefulness and suppressed during goal-driven behavior. We hypothesize that inhibitory interference with spontaneous ongoing, that is, not task-driven, activity in the angular gyrus (AG), one of the core regions of the default mode network, will enhance the dominant idling EEG alpha rhythms observed in the resting state. Fifteen right-handed healthy adult volunteers underwent to this study. Compared with sham stimulation, magnetic stimulation (1 Hz for 1 min) over both left and right AG, but not over FEF or intraparietal sulcus, core regions of the dorsal attention network, enhanced the dominant alpha power density (8–10 Hz) in occipitoparietal cortex. Furthermore, right AG-rTMS enhanced intrahemispheric alpha coherence (8–10 Hz). These results suggest that AG plays a causal role in the modulation of dominant low-frequency alpha rhythms in the resting-state condition. ■

INTRODUCTION

Alpha rhythms (about 8–12 Hz), first described by Berger (1929), are the most prominent feature in the EEG of a person in a state of quiet alert wakefulness (herein "resting state"). They have predominant occipitoparietal topography and are thought to correlate with cortical arousal and attenuated information processing. Alpha rhythms are possibly related to cortical inhibition induced by the synchronization of thalamic and cortical granular and pyramidal neurons (Bollimunta, Mo, Schroeder, & Ding, 2011; Pfurtscheller & Lopes da Silva, 1999; Steriade, Datta, Paré, Oakson, & Curró Dossi, 1990).

The resting brain, as seen through the lens of fMRI, is characterized by low-frequency (about 0.1 Hz) fluctuations of the blood oxygenation signal (BOLD) that are temporally correlated across large-scale distributed networks resembling those activated during task performance (Deco & Corbetta, 2011; Smith et al., 2009; Fox & Raichle, 2007; Biswal, DeYoe, & Hyde, 1996). One of these networks, the default mode network (DMN), originally identified as a set of parietal and medial frontotemporal regions consistently suppressed during goal-driven behavior (Shulman et al., 1997), was noted to have tonically increased metabolic activity (Raichle et al., 2001), especially glycolythic consumption (Vaishnavi et al., 2010). Although many and disparate cognitive functions, including self-referential autobiographical processing (Dastjerdi et al., 2011), memory retrieval (Sestieri, Corbetta, Romani, & Shulman, 2011; Sestieri, Shulman, & Corbetta, 2010), simulation of future events (Buckner, Andrews-Hanna, & Schacter, 2008), and suppression of irrelevant sensory events (Chadick & Gazzaley, 2011; Lewis, Baldassarre, Committeri, Romani, & Corbetta, 2009), have been proposed for the DMN, its functional importance during quiet resting wakefulness is undisputed. Also, notably, the DMN shows a competitive relationship both at rest (Fox et al., 2005) and during attention and memory tasks (Sestieri et al., 2010) with the so-called dorsal attention network (DAN; Corbetta & Shulman, 2002, 2011), a set of frontoparietal regions involved in the selection of behaviorally relevant sensory-motor information. For instance, during visual selection tasks, the DAN is strongly recruited while the DMN is suppressed, whereas during retrieval of memory information, the reverse occurs (Sestieri et al., 2010).

The relationship between activity in the DMN and alpha band power in the awake restful state has been investigated with conflicting results by recording simultaneously EEG rhythms and fMRI BOLD signals. Although one study found a positive correlation between fluctuations of the BOLD signals in the DMN at rest and alpha power fluctuations (Mantini, Perrucci, Del Gratta, Romani, & Corbetta, 2007), others reported either weak or no correlation (Knyazev, Slobodskoj-Plusnin, Bocharov, & Pylkova, 2011; Wu, Eichele, & Calhoun, 2010; Gonçalves et al., 2006; Laufs et al., 2003). In contrast, more consistent and robust negative correlations have been reported between BOLD signal fluctuations in the DAN and alpha power (Sadaghiani et al., 2010; Mantini et al., 2007; Laufs et al., 2003) and BOLD signal fluctuations in the DMN

[1]University G. D'Annunzio, Chieti, Italy, [2]University of Rome La Sapienza, Rome, Italy, [3]IRCCS San Raffaele Pisana, Rome, Italy, [4]Washington University School of Medicine in St. Louis, MO

Journal of Cognitive Neuroscience 26:1, pp. 107–119
doi:10.1162/jocn_a_00460

and beta power (Mantini et al., 2007; Laufs et al., 2003). This brief review indicates that the relationship between BOLD signal fluctuations in specific cortical networks and EEG rhythms is complex.

Correlations between fMRI BOLD and EEG signals are quite interesting but provide only indirect evidence for a causal relationship between these two sets of signals. More direct evidence about the generation or modulation of cortical rhythms can be obtained by examining the effects of excitatory or inhibitory repetitive TMS (rTMS) to a given cortical region onto the ongoing EEG rhythms.

We have recently used this method to study the causal role of dorsal attention regions, intraparietal sulcus (IPS), and FEF, in the control of anticipatory (pretarget) occipitoparietal alpha desynchronization, a putative correlate of top–down attention control (Capotosto, Babiloni, Romani, & Corbetta, 2009, 2012). Interference with IPS and FEF preparatory activity following a spatial cue induced an abnormal enhancement of alpha rhythms in the occipitalparietal region contralateral to the expected visual stimuli, consistent with a disruption of top–down modulation (Capotosto, Babiloni, et al., 2012; Capotosto et al., 2009).

Here, we test the role of a core region of the DMN, the angular gyrus (AG), in the modulation of alpha rhythms under the assumption that this region is spontaneously active during rest (Raichle et al., 2001) and that mediates ongoing internally directed cognitive processes (Sestieri et al., 2010). Accordingly, suppression of AG by rTMS at rest should produce, as in the case of DAN regions during attention, an abnormal increase in alpha power in posterior cortical regions where alpha rhythms are typically dominant in the resting-state condition. Furthermore, the propagation of the inhibitory enhancement of alpha rhythms are expected to be preponderant in the hemisphere ipsilateral to TMS interference, because of the well-known, more efficient functional connectivity within any hemisphere. To ascertain the location and frequency specificity of these effects and in relation to the inverse relationship between alpha and beta rhythms and BOLD fluctuations, respectively, in the DAN (Sadaghiani et al., 2010; Mantini et al., 2007; Laufs et al., 2003) and DMN (Mantini et al., 2007; Laufs et al., 2003), core nodes of the DAN (IPS, FEF) were also tested, and the frequency analysis was extended to both alpha and beta bands.

METHODS

Participants

Fifteen right-handed (Edinburgh Inventory) healthy adult volunteers (age range = 21–27 years old, six women) with no previous psychiatric or neurological history participated in the experiment. Their vision was normal or corrected-to-normal. All experiments were conducted with the understanding and written consent of each participant according to the Code of Ethics of the World Medical Association and the standards established by the University of Chieti Institutional Review Board and Ethics Committee.

Experimental Task

All measurements were carried out at the Institute of Technology and Advanced Bioimaging by the first author (P. C.). Participants were seated in a comfortable reclining armchair. They maintained fixation on a small white cross stimulus (subtending 0.7° of visual angle) displayed on a black background in the center of a computer screen positioned at a distance of 80 cm.

Procedures for rTMS and Identification of Target Scalp Regions

rTMS was used to interfere with neural activity. The stimulation was delivered through a focal, figure-eight coil (outer diameter of each wing 7 cm) connected with a standard Mag-Stim Rapid 2 stimulator (Carmarthenshire, UK; maximum output = 2.2 T). A mechanical arm maintained the handle of the coil angled at about 45° away from the midline. The exact position was adjusted based on the results of the on-line neuronavigation such that the center of the coil wing was oriented perpendicularly to the point to be stimulated with the maximum power. The center of the coil wings was positioned at a position on the scalp corresponding to each cortical ROI. Individual resting excitability threshold for right motor cortex stimulation was preliminarily determined by following standardized procedures (Rossini et al., 1994). The rTMS train was delivered based on the following parameters: 1-min duration, 1-Hz frequency, and intensity set at 100% of the individual motor threshold. These parameters are consistent with published safety guidelines for TMS stimulation (Rossi, Hallett, Rossini, & Pascual-Leone, 2009; Anderson et al., 2006; Machii, Cohen, Ramos-Estebanez, & Pascual-Leone, 2006; Wassermann, 1998). Of note, 1-Hz rTMS for 1 min is thought to inhibit the target cortical area for 1 or 2 min poststimulation.

The experimental design included seven conditions, applied in different blocks, and randomized across participants. Each participant performed all the conditions. Two consecutive TMS sessions were separated by an interval of about 5 min. In the Sham condition, the stimulation was delivered at the scalp vertex with the position of the coil reversed with respect to the scalp surface, such that the magnetic flux was dispersed in the air. In the six active conditions, the center of the coil wings was positioned at a position on the scalp corresponding to different cortical regions obtained from a meta-analysis of spatial attention studies (He et al., 2007; Fox et al., 2005). Four of these regions corresponded to core regions of the DAN: right pIPS (x, y, z: 23, −65, 48), left pIPS (x, y, z: −25, −63, 47), right FEF (x, y, z: 32, −9, 48), left FEF (x, y, z: 26, −9, 48). The two other regions

are hubs of the DMN: right AG (x, y, z: 53, −67, 46), left AG (x, y, z: −47, −67, 36). The positioning of the TMS coil onto the participants' scalp was based on a procedure developed as part of the SofTaxic software that allows to reconstruct an individualized head model based on a set of digitized skull landmarks (nasion, inion, and two preauricular points) and on about 40 scalp points entered with a Fastrak Polhemus digitizer system (Polhemus). Such model is then warped to a standard mean MRI-based head template (152 participants, SPM tool version 2) through affine linear transformation. The present procedure has been successful in previous rTMS studies (Sestieri, Capotosto, Tosoni, Romani, & Corbetta, 2013; Capotosto, Babiloni, et al., 2012; Capotosto, Corbetta, Romani, & Babiloni, 2012; Candidi, Stienen, Aglioti, & de Gelder, 2011; Capotosto et al., 2009; Harris, Benito, Ruzzoli, & Miniussi, 2008; Urgesi, Calvo-Merino, Haggard, & Aglioti, 2007; Babiloni, Vecchio, Miriello, Romani, & Rossini, 2006; Urgesi, Berlucchi, & Aglioti, 2004). Of note, whereas in our pilot studies we observed that rTMS over a ventral region (i.e., right TPJ, mean coordinates $x = 52$, $z = -49$, and $y = 17$) caused scalp and face muscular twitches and participants' discomfort, in this study none of the participants declared any kind of discomfort (i.e., pain) during each experimental conditions.

Electroencephalography Recordings

EEG data were recorded (BrainAmp, Gilching, Germany; bandpass, 0.05–100 Hz; sampling rate, 256 Hz) from 27 EEG electrodes placed according to an augmented 10–20 system and mounted on an elastic cap resistant to magnetic pulses. Electrode impedance was below 5 K. The artifact of rTMS on the EEG activity lasted about 10 msec and did not generate any alteration in the power spectrum. Two electrooculographic channels were used to monitor eye movement and blinking. The acquisition time for all conditions was set from −1.5 to +0 min before rTMS train onset and from +1 to +3 min after the rTMS train onset. EEG data were segmented off-line in windows of 2 sec. The intensive experimental design (six active TMS condition and one sham) imposed this limitation in the time extension of the rTMS and of the poststimulation periods to minimize fatigue and drops of vigilance. The EEG single trials contaminated by eye movement, blinking, or involuntary motor acts (e.g., mouth, head, trunk, or arm movements) were rejected off-line. To remove the effects of the electric reference, EEG single trials were rereferenced by the common average reference. The common average procedure includes the averaging of amplitude values at all electrodes and the subtraction of the mean value from the amplitude values at each single electrode.

The EEG data analysis was performed in the following periods of interest: (i) pre-TMS (1.5 min before rTMS train and off-line segmented in windows of 2 sec), (ii) post-TMS 1 (the first minute after rTMS train and off-line segmented in windows of 2 sec), and (iii) post-TMS 2 (the second minute after rTMS train and off-line segmented in windows of 2 sec). The mean number of trials per EEG segments of 2 sec was 42 (±3) for the pre-TMS period and 86 (±4) for the post-TMS period. Of note, EEG data sets of one participant were excluded because the profile of EEG power density spectra was clearly abnormal/artifactual in several TMS conditions.

Analysis of EEG Power

We measured the effect of rTMS at different cortical loci on the power of alpha and beta rhythms in parieto-occipital cortex. The EEG power, in a matrix of scalp electrodes, reflects the spatial and temporal summation of synchronous activity of cortical neurons whose synaptic currents are associated to changes of the voltage at those electrodes. For the EEG spectral analysis, two subbands of alpha rhythms were used, namely low- and high-frequency alpha. These subbands were determined in accordance to a standard procedure based on the peak of individual alpha frequency (IAF; Klimesch, Doppelmayr, Russegger, Pachinger, & Schwaiger, 1998). With respect to the IAF, these frequency bands were defined as follows: (i) low-alpha, IAF − 2 Hz to IAF, and (ii) high-alpha, IAF to IAF + 2 Hz. Moreover, with respect to the individual beta frequency (IBF) peak, for the EEG spectral analysis, we also used two subbands of beta rhythms, namely, low- and high-frequency beta, defined as follows: (i) low-beta, IBF − 2 Hz to IBF, and (ii) high-beta, IBF to IBF + 2 Hz. Of note, mean IAF peak across participants was 10.1 Hz (±0.2 *SE*), and mean IBF peak across participants was 18.9 Hz (±0.5 *SE*). No statistically significant difference was observed across the rTMS conditions ($p > .05$) for both alpha and beta peaks.

Estimation of the Functional Connectivity: Between-electrode Coherence Analysis

The effect of rTMS at different cortical loci was also tested on the coherence of alpha and beta rhythms at electrode pairs as an estimation of the functional coupling of EEG rhythms at different cortical sites. Spectral coherence is a normalized measure of the coupling between two (EEG) signals at any given frequency (Pfurtscheller & Andrew, 1999; Rappelsberger & Petsche, 1988). The coherence values were calculated for each frequency bin by the following equation:

$$\mathrm{Cohxy}(\ddot{e}) = |\mathrm{Rxy}(\ddot{e})|^2 = |\mathrm{fxy}(\ddot{e})|^2 / [\mathrm{fxx}(\ddot{e})\mathrm{fyy}(\ddot{e})]$$

This equation is the extension of the Pearson's correlation coefficient to complex number pairs. In this equation, f denotes the spectral estimate of two EEG signals x and y for a given frequency bin (ë). The numerator contains

the cross-spectrum for x and y (fxy), whereas the denominator contains the respective autospectra for x (fxx) and y (fyy). For each frequency bin (ë), the coherence value (Cohxy) is obtained by squaring the magnitude of the complex correlation coefficient R. This procedure returns a real number between 0 (no coherence) and 1 (max coherence).

For the evaluation of the interhemispheric spectral coherence, the electrode pairs were F3–F4 (frontal areas), C3–C4 (central areas), P7–P8 (parietal areas), O1–O2 (occipital areas), and T7–T8 (temporal areas). For the evaluation of the intrahemispheric spectral coherence, the electrode pairs were F3–P3 (frontoparietal), F3–O1 (fronto-occipital), and F3–T3 (frontotemporal) for the left hemisphere and F4–P4 (frontoparietal), F4–O2 (fronto-occipital), and F4–T4 (frontotemporal) for the right hemisphere. The coherence of the EEG data was computed in the baseline pre-TMS period and in the poststimulus period (namely, Post-TMS 1 and Post-TMS 2) for the mentioned seven conditions (i.e., Sham, Left-AG, Right-AG, Left-IPS, Right-IPS, Left-FEF, and Right-FEF).

Of note, EEG coherence is not mathematically independent of power of the EEG signal at electrode sites, as they result from the computation of fast Fourier transform. However, the two indexes do not provide redundant information. For example, the alpha power in a matrix of scalp electrodes reflects the spatial and temporal summation of synchronous activity of cortical neurons at about 10 Hz whose synaptic currents are associated to changes of the voltage at those electrodes. Alpha coherence among pairs of those electrodes is related to the linear interdependence of the alpha rhythms among specific pairs of electrodes. More analytically, consider the case in which the electrodes A, B, and C of the matrix have the same amount of alpha power. The coherence in alpha band between the electrode A and the two electrodes B and C can be markedly different as a function of relative distance and underlying structural brain connectivity. Keeping in mind these considerations, one cannot predict the amplitude of the EEG coherence between electrode pairs only on the basis of EEG power at the corresponding electrodes.

Statistical Analysis

Statistical comparisons were performed by repeated-measures ANOVAs. We used Mauchley's test to evaluate the sphericity assumption of the ANOVA, a Greenhouse–Geisser procedure for the correction of the degrees of freedom, and Duncan tests for post hoc comparisons ($p < .05$).

The ANOVAs aimed at unveiling the most effective sites of rTMS stimulation and the topographical localization of the most important effects on alpha rhythms. Because of the relatively small population size, separate simple ANOVA designs were used for alpha subbands (low and high frequency) and TMS sites. For the ANOVAs using EEG Power Density as a dependent variable, Time (Pre-TMS, Post-TMS 1, Post-TMS 2) and Electrode (F3, F4, C3, C4, T7, T8, P7, P8, O1, O2) served as within-subject factors. For the ANOVAs using spectral coherence as a dependent variable, Topology (Interhemispheric, Right Intrahemispheric, and Left Intrahemispheric) and Time (Pre-TMS, Post-TMS 1, Post-TMS 2) served as within-subject factors. The interhemispheric coherence was defined as the mean of the coherence values across frontal (F3–F4), central (C3–C4), parietal (P7–P8), temporal (T7–T8), and occipital (O1–O2) electrode pairs. For the left intrahemispheric coherence, the coherence values were averaged across frontoparietal (F3–P3), fronto-occipital (F3–O1), and frontotemporal (F3–T3). For the right intrahemispheric coherence, the coherence values were averaged across frontoparietal (F4–P4), fronto-occipital (F4–O2), and frontotemporal (F4–T4).

Considering the amount of factors (i.e., Time and Electrode), relative levels and population size, an ANOVA design including all TMS sites would have been inappropriate as a main statistical analysis. Nevertheless, we performed an exploratory analysis to directly compare the effects of the rTMS over DMN and DAN networks on posterior resting-state EEG rhythms. Specifically, we computed two exploratory ANOVAs, one using EEG power density as a dependent variable and the other using spectral coherence. In the first exploratory ANOVA, we averaged the alpha power values across selected parieto-occipital electrodes (i.e., P7, P8, O1, O2) and the rTMS conditions relative to a single cortical network (i.e., DMN, DAN). For the DMN, the alpha power density for the left and right AG was averaged. For the DAN, the alpha power density for bilateral IPS and FEF was averaged. On the whole, the first exploratory ANOVA included Network (DMN and DAN; independent variable) and Time (Pre-TMS, Post-TMS 1, Post-TMS 2) as within-subject factors. In the second exploratory ANOVA, we averaged the alpha coherence across all electrode pairs and the rTMS conditions relative to a single cortical network as well. For the DMN, the alpha coherence for the left and right AG was averaged. For the DAN, the alpha coherence for bilateral IPS and FEF was averaged. On the whole, the second exploratory ANOVA included Network (DMN and DAN; independent variable), Hemisphere (ipsilateral or contralateral to the stimulation), and Time (Pre-TMS, Post-TMS 1, Post-TMS 2) as within-subject factors.

To test the frequency-specific effect of rTMS on the alpha rhythms, we performed an analogue analysis on beta power and coherence. Separate ANOVAs were designed for beta subbands (low- and high-frequency) and TMS sites. For the ANOVAs using EEG Beta Band Power Density as a dependent variable, Time (Pre-TMS, Post-TMS 1, Post-TMS 2) and Electrode (F3, F4, C3, C4, T7, T8, P7, P8, O1, O2) served as within-subject factors. For the ANOVAs using spectral beta coherence as a dependent variable, Topology (Interhemispheric, Right Intrahemispheric, and Left Intrahemispheric) and Time

(Pre-TMS, Post-TMS 1, Post-TMS 2) served as within-subject factors. Furthermore, to directly compare the effect of the rTMS over DMN and DAN, we used ANOVAs for the beta band (averaging low and high beta) in line with those used for the analysis of the alpha band.

To rule out effects of rTMS on baseline alpha power (pre-TMS period), two ANOVAs used Condition (Sham, Right-AG, Left-AG, Right-IPS, Left-IPS, Right-FEF, Left-FEF) and Electrode (F3, F4, C3, C4, T7, T8, P7, P8, O1, O2) as within-subject factors. The two ANOVAs were focused on low- and high-frequency alpha subbands, respectively.

RESULTS

Alpha Power Density

Figure 1A shows the topographic maps of low- and high-frequency alpha power density in the Sham condition during the three periods of interest (Pre-TMS, Post-TMS 1, Post-TMS 2). Figure 1B shows the mean alpha power density, separately for low and high alpha, in different electrodes and periods of interest. Resting-state alpha power density was higher in amplitude over the parieto-occipital regions in all periods of interest, and Sham stimulation did not produce any significant modulation ($p > .05$). This analysis rules out any consistent effect of Sham or other experimental procedures on the resting-state alpha rhythms.

Figure 2 shows the low-frequency alpha power density for Right-AG, Left-AG, Right-IPS, Left-IPS, Right-FEF, and Left-FEF conditions during the three periods of interest (Pre-TMS, Post-TMS 1, Post-TMS 2), respectively. In all conditions, the resting-state alpha power density was higher in amplitude at bilateral parietal and occipital electrodes. At these electrodes, right AG stimulation induced a progressive increase of alpha power in the

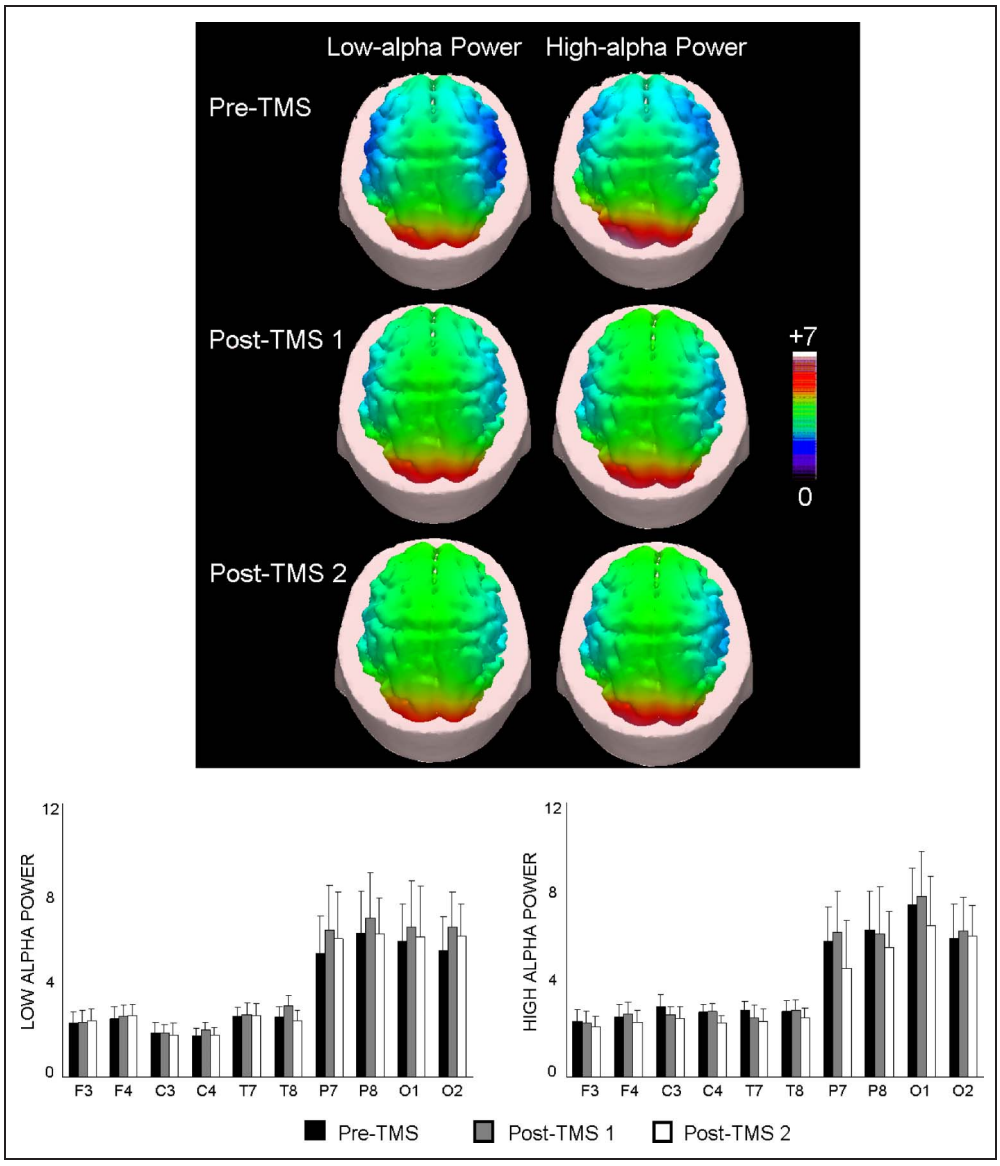

Figure 1. Topography of low- and high-frequency alpha power density in the Sham condition. (Top) Topographic maps of low- and high-frequency alpha power density during the three periods of interest (Pre-TMS, Post-TMS 1, Post-TMS 2). (Bottom) Group means (±*SE*) of the low- and high-frequency alpha power density in the Sham condition.

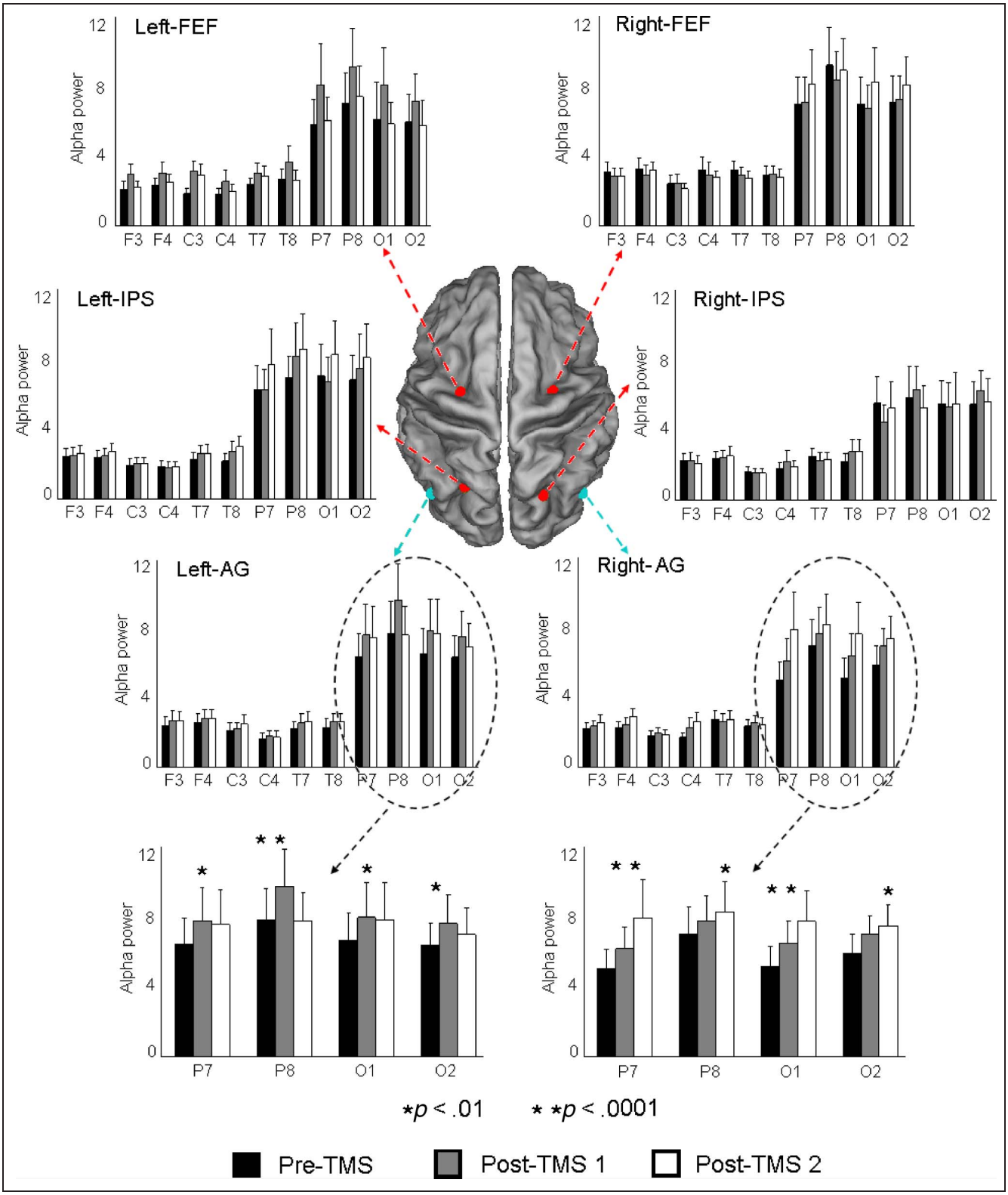

Figure 2. Alpha power density: Group means (±*SE*) of the low-frequency alpha power density for all active magnetic stimulation sites (i.e., Right-AG, Left-AG, Right-IPS, Left-IPS, Right-FEF, Left-FEF) and periods of interest (pre-TMS, post-TMS 1, post-TMS 2). Duncan post hoc test: Statistically significant differences between pre- and post-TMS periods are indicated by one ($p < .01$) or two ($p < .0001$) asterisks.

first (Post-TMS 1) and second minute (Post-TMS 2) after stimulation. This impression was confirmed by a statistical analysis showing a significant interaction between Time and Electrode factors for right AG, $F(18, 234) = 1.85$, $p < .02$. Post hoc tests indicated an increment of low-frequency alpha power density at occipital-parietal electrodes during the post-TMS 1 (P7 $p < .05$; O1 $p < .03$) and post-TMS 2 periods (P7 $p < .0001$; P8 $p < .05$; O1 $p < .0001$; O2 $p < .01$; Figure 2). A similar effect was also observed for left AG, $F(18, 234) = 1.64$, $p < .05$, stimulation condition. Post hoc tests indicated an increment of low-frequency alpha power density at occipital-parietal electrodes during the post-TMS 1 (P7 $p < .01$; P8 $p < .0001$; O1 $p < .01$; O2 $p < .02$) and post-TMS 2 periods (P7 $p < .02$; O1 $p < .04$; O2 $p < .01$; Figure 2). These increments were not observed at the high-frequency alpha subband. These findings were found to be specific for the stimulation of DMN. Statistical analysis showed no significant effect of rTMS over Right-IPS, Left-IPS, Right-FEF, and Left-FEF (i.e., DAN) on alpha power density ($p > .05$).

Finally, a control analysis for each condition was performed to test the main effect Time on the low-frequency alpha power density. With respect to the ANOVAs of the main analysis, the same within-subject factors were used. As a difference, only the parieto-occipital electrodes of interest (i.e., P7, P8, O1, O2) were used. We observed that only the inhibitory rTMS over right AG produced a main effect Time, $F(2, 26) = 3.62$, $p < .04$, whereas the rTMS over left AG produced a marginal statistical effect, $F(2, 26) = 3.10$, $p = .06$, thus globally confirming the results of the main analysis.

Alpha Spectral Coherence

In line with the results of alpha power density, Sham stimulation produced no statistically significant effect on alpha coherence ($p > .05$).

Figure 3 shows the low-frequency mean alpha coherence for Right-AG, Left-AG, Right-IPS, Left-IPS, Right-FEF, and Left-FEF conditions during the three periods of interest (Pre-TMS, Post-TMS 1, Post-TMS 2), respectively. The alpha coherence values were averaged across electrode pairs to index interhemispheric, left intrahemispheric, and right intrahemispheric coherence (see Methods). In all conditions mean coherence was higher in inter- than intrahemispherical indexes regardless of rTMS conditions ($p < .001$). For these indexes, right AG stimulation induced a progressive increase of alpha coherence along Post-TMS 1 and Post-TMS 2 periods. Again, statistical analysis showed that the only remarkable effect of the rTMS on alpha coherence was observed for the magnetic stimulation of DMN but not DAN. Only for the stimulation of right AG, there were statistically significant effects. Specifically, there was an interaction between Topology and Time factors, $F(4, 52) = 3.05$, $p < .03$, indicating the increase of the right intrahemispheric low-frequency alpha coherence during post-TMS 1 and post-TMS 2 ($p < .0001$). A mirror effect of left AG stimulation on the left intrahemispheric low-frequency alpha coherence did not reach the statistical significance ($p > .05$). These increments were not observed in the high-frequency alpha subband.

Finally, control ANOVAs considering separately each Topology of the coherence (i.e., right hemisphere, left hemisphere) were computed to the main effect Time. The results of the main analysis were confirmed. In particular, an ANOVA using right intrahemispheric coherence (i.e., ipsilateral to the stimulation) as a dependent variable and Time (Pre-TMS, Post-TMS 1, Post-TMS 2) as within-subject factor showed a main effect of Time for the rTMS over right AG, $F(2, 26) = 3.57$, $p = .04$. Post hoc test indicated an increase of the right intrahemispheric low-frequency alpha coherence during post-TMS ($p < .02$). The counterpart using left intrahemispheric coherence (i.e., ipsilateral to the stimulation) as a dependent variable only provided statistically marginal results, $F(2, 26) = 2.69$, $p = .08$.

DMN versus DAN

To compare the effect of rTMS over the two networks on the low-frequency alpha power density, we performed an ANOVA with Network (DMN, DAN; after averaging over nodes), Hemisphere (Left, Right), and Time (Pre-TMS, Post-TMS 1, Post-TMS 2). Figure 4A shows the low-frequency mean alpha power density for DMN (after averaging Right-AG and Left-AG) and DAN (after averaging Right-IPS, Left-IPS, Right-FEF, and Left-FEF) during the three periods of interest (Pre-TMS, Post-TMS 1, Post-TMS 2), respectively. Although the interaction between Networks and Time did not reach the statistical significance ($p = .085$), rTMS over DMN induced a progressive increase of the alpha power in the first (Post-TMS 1) and in the second minute (Post-TMS 2) after magnetic stimulation. This effect was not observed for rTMS over DAN.

Figure 4B shows the low-frequency mean alpha coherence for DMN (after averaging Right-AG and Left-AG) and DAN (after averaging Right-IPS, Left-IPS, Right-FEF, and Left-FEF) during the three periods of interest (Pre-TMS, Post-TMS 1, Post-TMS 2), respectively, separated by Hemisphere (ipsilateral or contralateral to the stimulation). Statistical analysis showed that the only significant effect of the rTMS on alpha coherence was observed for the magnetic stimulation of DMN (AG) but not DAN. Specifically, there was an interaction between Network and Time, $F(2, 26) = 3.21$, $p = .05$, and an interaction between Network, Hemisphere, and Time factors, $F(2, 26) = 4.58$, $p = .02$, indicating that DMN (AG) magnetic stimulation induced a progressive increase of the ipsilateral intrahemispheric low-frequency alpha coherence during post-TMS 1 and post-TMS 2 ($p < .0001$). A similar trend was also observed stimulating DMN for the contralateral intrahemispheric low-frequency alpha coherence.

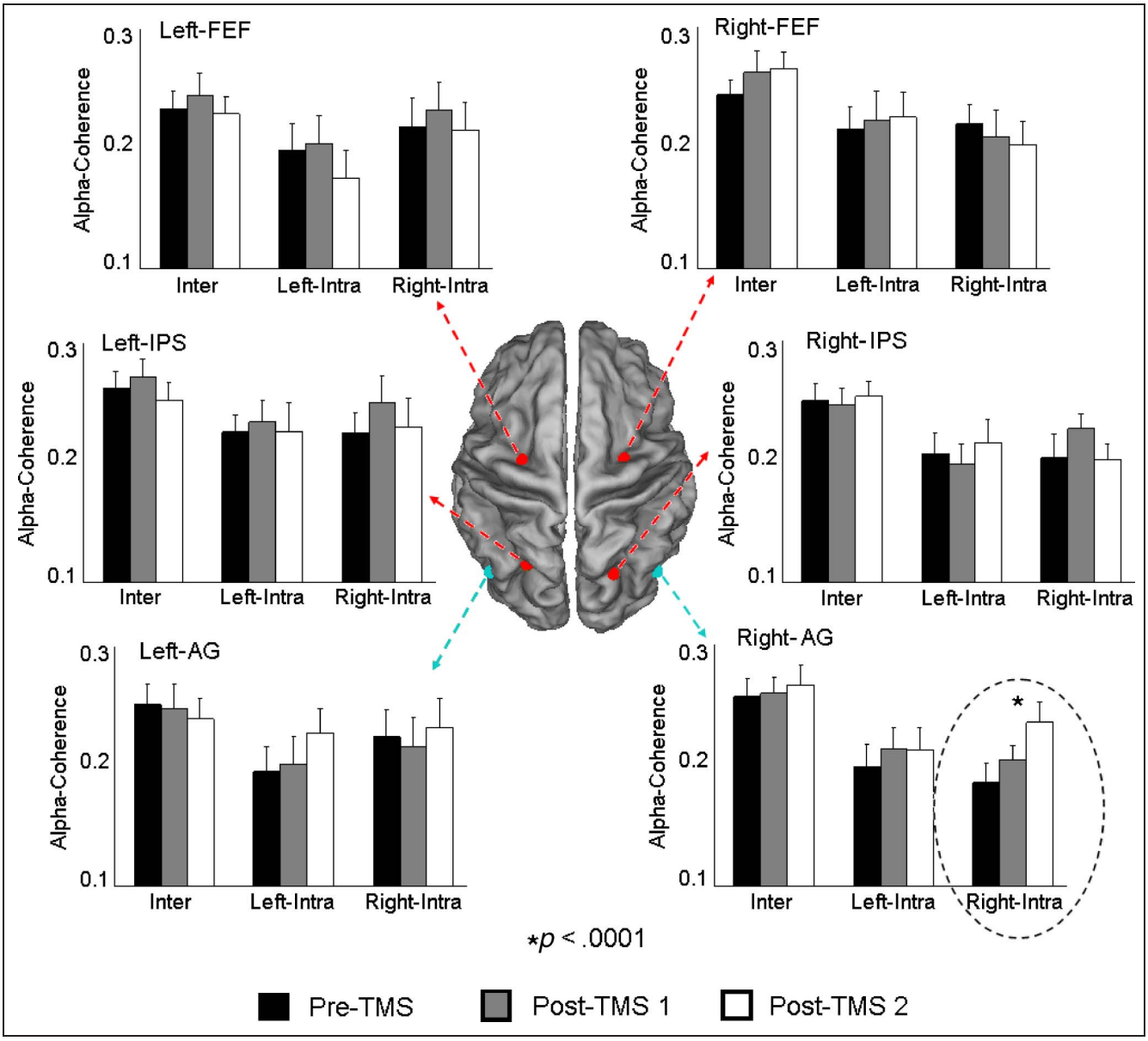

Figure 3. Alpha coherence: Group means (±*SE*) of the low-frequency alpha inter- and intrahemispheric coherence for all active magnetic stimulation sites (i.e., Right-AG, Left-AG, Right-IPS, Left-IPS, Right-FEF, Left-FEF) and periods of interest (pre-TMS, post-TMS 1, post-TMS 2). Duncan post hoc test: Statistically significant differences between pre- and post-TMS periods are indicated by one asterisk ($p < .0001$).

Of note, no statistically significant results were observed for both power and coherence in the high frequency alpha subband.

Beta Power Density and Spectral Coherence

For both low- and high-beta power and coherence, no statistically significant interaction was observed for the interference of rTMS ($p > .05$). The same lack of statistical effects ($p > .05$) was observed when DMN and DAN were compared in the beta band (Figure 5). There was only a trend similar to that observed in the alpha band, especially for the EEG coherence ipsilateral to the stimulation site (e.g., right AG). These results suggest a more strict causal relationship between AG and the modulation of alpha compared with beta rhythms in the resting-state condition.

Control Analyses

Control statistical analysis showed no significant difference of the alpha power density in the pre-TMS period (baseline) among Sham, Right-AG, Left-AG, Right-IPS, Left-IPS, Right-FEF, and Left-FEF conditions ($p > .05$). This was true for both low- and high-frequency alpha subbands. These finding confirmed that the main results were not because of different baseline alpha power density among the conditions of magnetic stimulation.

DISCUSSION

There exists a classic relationship between a state of resting wakefulness and the presence of a dominant alpha rhythm on the EEG (Berger, 1929). More recently, the resting state has been associated with tonic metabolic and neural activity in the DMN, a distributed fronto-temporal-parietal cortical network active at rest (Vaishnavi et al., 2010; Raichle et al., 2001). We tested the hypothesis that AG plays a causal role in the modulation of resting-state alpha rhythms in the posterior cortical regions under the assumption that DMN regions are active in the resting state possibly in support of internally directed cognition (Sestieri et al., 2010). In agreement with this hypothesis, we found that inhibitory (1 Hz) rTMS stimulation of the AG for 1 min enhanced alpha power in both hemispheres in the poststimulus period (i.e., first and second minute poststimulation). This modulation was stronger for right AG stimulation, which also produced increased alpha spectral coherence ipsilaterally in the right hemisphere. Critically these effects were specific for AG. Sham stimulation and magnetic stimulation of two nodes of the DAN (i.e., FEF and IPS on either hemisphere) did not produce any significant modulation of alpha power or coherence. In addition, the modulation was also not only location specific but also frequency specific to the low frequency alpha rhythms (8–10 Hz) and did not extend to the high-frequency alpha rhythms (10–12 Hz). This is consistent with a model in which different frequencies of alpha rhythms reflect different functional modes of thalamo-cortical and cortico-cortical loops that facilitate/inhibit the transmission and retrieval of sensorimotor and cognitive information (Pfurtscheller & Lopes da Silva, 1999).

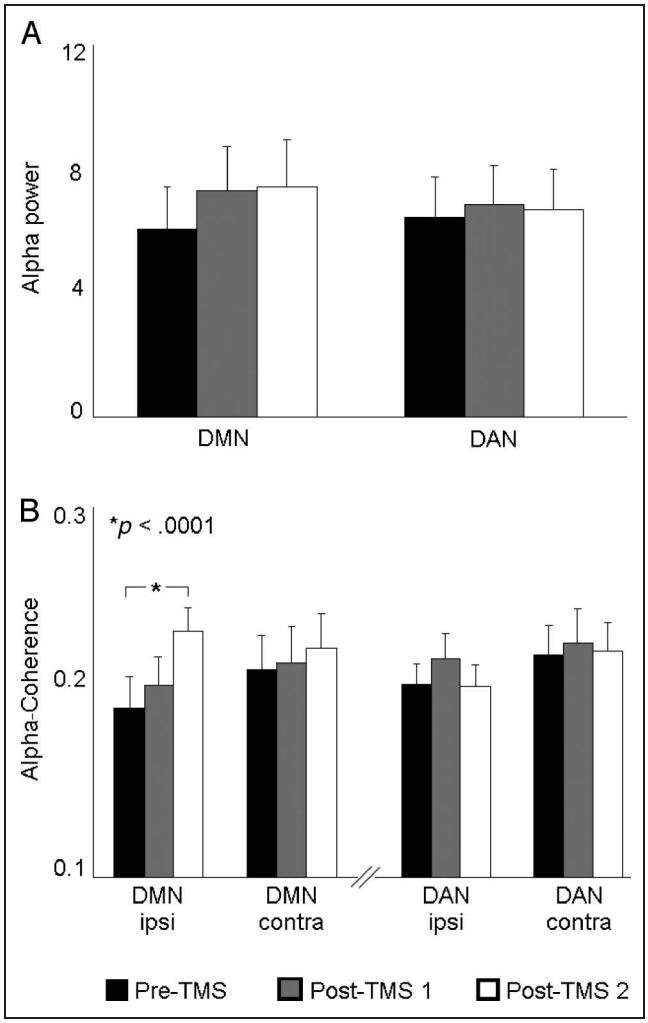

Figure 4. DMN versus DAN in the alpha band: (A) Group means (±*SE*) of the low-frequency alpha power density for the two networks (DMN and DAN) and periods of interest (pre-TMS, post-TMS 1, post-TMS 2). (B) Group means (±*SE*) of the low-frequency alpha intrahemispheric coherence for the two networks (DMN and DAN) and periods of interest (pre-TMS, post-TMS 1, post-TMS 2), separated by Hemisphere (ipsilateral and contralateral to the stimulation). Duncan post hoc test: Statistically significant differences between pre- and post-TMS periods are indicated by one asterisk ($p < .0001$).

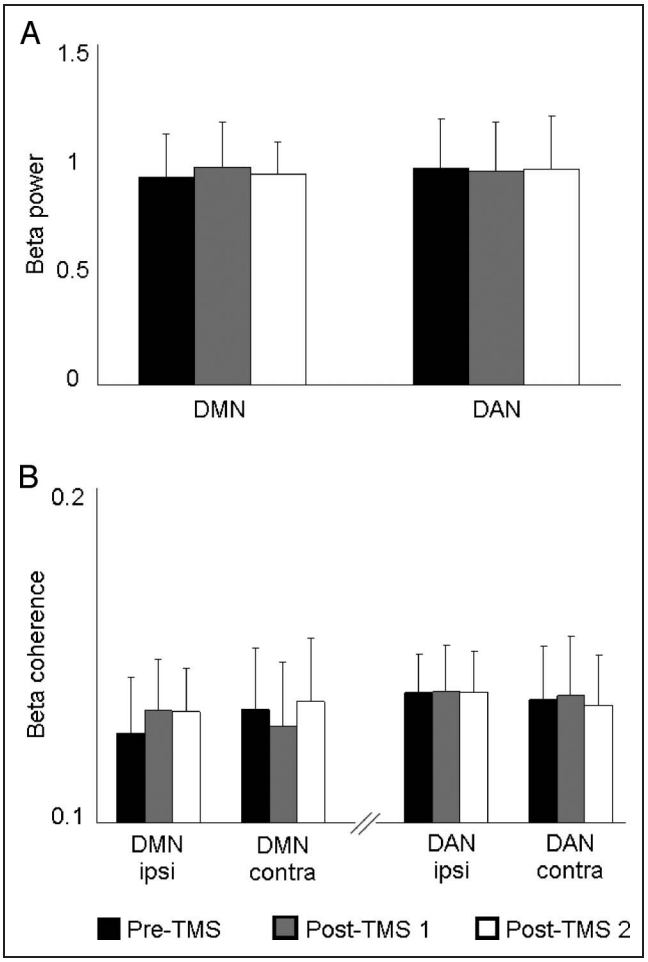

Figure 5. DMN versus DAN in the beta band: (A) Group means (±*SE*) of the beta power density for the two networks (DMN and DAN) and periods of interest (pre-TMS, post-TMS 1, post-TMS 2). (B) Group means (±*SE*) of the beta intrahemispheric coherence for the two networks (DMN and DAN) and periods of interest (pre-TMS, post-TMS 1, post-TMS 2), separated by Hemisphere (ipsilateral and contralateral to the stimulation).

Specifically, it has been proposed that low-frequency alpha rhythms would diffusely regulate global brain arousal and alertness, whereas high-frequency alpha rhythms would reflect task-related oscillations of selective neural systems involved in the elaboration of task-specific information (Klimesch et al., 1998). The frequency-specific effect of rTMS over DMN was further supported by a lack of modulation in the beta band.

Overall these findings albeit exploratory strongly suggest a direct "causal" link between activity in the AG at rest and modulation/generation of alpha rhythms. Several open question remains.

One question concerns the physiological mechanisms underlying this modulation. Repeated 1-Hz stimulation of neocortex by rTMS is thought to cause a (partial) suppression of excitatory synaptic transmission (Ridding & Ziemann, 2010; Thickbroom, 2007) and induces long-term specific changes in the expression of c-Fos (Funke & Benali, 2010; Aydin-Abidin, Trippe, Funke, Eysel, & Benali, 2008) and GABA-synthesizing enzymes (Funke & Benali, 2010; Trippe, Mix, Aydin-Abidin, Funke, & Benali, 2009). A reduction in calcium-binding protein calbindin in inhibitory interneurons modulating the activity of pyramidal cells has been also reported. Therefore, 1-Hz TMS stimulation is expected to tonically suppress neuronal activity. On the basis of our study, the effect extended for 2 min following 1-min stimulation in AG. We selected our stimulation and poststimulation periods based on an important study that showed that low-frequency (i.e., 1 Hz) rTMS over motor cortex induces an inhibitory enhancement of the alpha rhythms for a period corresponding to that of the magnetic stimulation (Brignani, Manganotti, Rossini, & Miniussi, 2008). Interestingly, in our study modulation of alpha power extended significantly into the second minute poststimulation suggesting that AG suppression is more prolonged than motor cortex. This may be because of the more central position of AG in the neuroanatomical matrix of connections and networks (see below; Buckner et al., 2009; Hagmann et al., 2008). Follow-up studies will need to trace the time course of this tonic inhibition, thus also allowing a full recovery of the effects to baseline and the reconstruction of the timing of the effect peak and plateau. Furthermore, they may include an active control TMS condition targeting scalp vertex (a region here used as Sham) as a site where TMS elicits no muscle activation (Mutanen, Mäki, & Ilmoniemi, 2013). The relative results would refine the understanding of the neural basis of the present results, although we did not observe any remarkable discomfort or muscle interference stimulating over regions of DAN and DMN.

Because cortical alpha rhythms are presumed to be generated by the oscillatory activity of granular and pyramidal neurons, mainly based on the input signals delivered by relay mode and high-threshold bursting thalamo-cortical neurons (Bollimunta et al., 2011; Lorincz, Kékesi, Juhász, Crunelli, & Hughes, 2009), our results suggest that suppression of AG activity modulated either cortical parieto-occipital regions where alpha rhythms localize or their thalamo-cortical inputs.

The modulation of alpha rhythms did not remain local but spread, especially for right AG stimulation, ipsilaterally across other cortical sites as demonstrated by a diffuse increased intrahemispheric coherence as compared with other cortical sites (e.g., IPS and FEF). One possible explanation for the increase in intrahemispheric coherence is the previously noted central position of AG in the structural/functional neuroanatomical matrix of the brain (Buckner et al., 2009; Hagmann et al., 2008). It is also consistent with recent magnetoencephalographic (MEG) evidence from our group showing that the DMN is a hub of inter-network cortical interactions in the resting state especially in the alpha and beta frequency bands (de Pasquale et al., 2012).

Another important question is the relationship of our results to the extant fMRI-EEG literature. The enhancement of alpha power after AG suppression is apparently in contradiction with some studies that find a positive relationship between alpha power and BOLD signal fluctuations in the DMN at rest (e.g., Mantini et al., 2007; but see Knyazev et al., 2011; Wu et al., 2010; Gonçalves et al., 2006; Laufs et al., 2003). Similarly, lack of modulation after suppression of DAN nodes (IPS, FEF) apparently contradicts the negative relationship between alpha power and BOLD signal fluctuations in the DAN at rest (Sadaghiani et al., 2010; Mantini et al., 2007; Laufs et al., 2003). However, one should consider the different timescale over which these effects are measured with different methods. In our study, effects were transient lasting for only a couple of minutes after stimulation. In contrast EEG/fMRI correlations are recorded and maintain significance over tens of minutes. Another major difference is the spatial resolution that is more precise with fMRI than EEG. For instance, it would be important to separate the direct effect of rTMS suppression on AG activity versus the indirect modulation on other regions. To this effect, it is important to underscore that scalp alpha rhythms reflect the summation of neural currents generated by different processes and cortical regions, including regions that are active hence desynchronized and regions that are relatively suppressed hence more synchronized. This summation at the scalp level might confound the interpretation of the "correlation" in EEG-fMRI studies.

A third issue concerns the functional significance of the alpha power/coherence enhancement after AG stimulation. Our interpretation assumes that posterior parieto-occipital alpha rhythm underlies a state of "idling" or partial inactivity of cortical information processing in relation to external stimuli. Task-related recruitment of cortex desynchronizes low/intermediate EEG frequencies including alpha and beta but synchronizes higher EEG frequencies including gamma (Friese, Supp, Hipp, Engel, & Gruber, 2012; Miller, Weaver, & Ojemann, 2009; Siegel, Donner, Oostenveld, Fries, & Engel, 2008; Canolty

et al., 2007; Freunberger et al., 2007; Crone, Sinai, & Korzeniewska, 2006). The degree of alpha synchronization in occipital-parietal sensory regions is putatively controlled during perceptual tasks by higher-order cortical regions involved in top–down control (Fries, 2005; Corbetta & Shulman, 2002). As a result, occipitoparietal alpha power is high in a state of idleness (rest), decreases during visual (attention) tasks (e.g., Thut, Nietzel, Brandt, & Pascual-Leone, 2006; Worden, Foxe, Wang, & Simpson, 2000), and paradoxically increases when regions of the DAN presumably controlling the allocation of attention are (partially) inactivated by inhibitory rTMS (Capotosto, Babiloni, et al., 2012; Capotosto et al., 2009).

By analogy, if the AG is involved in internally directed cognition such as memory retrieval (Sestieri et al., 2010) or simulation of the future, and these processes are spontaneously active at rest as suggested by metabolic studies (Raichle et al., 2001), then inactivation of AG is expected to cause a local inhibitory increase in alpha power as well as a propagation of such perturbation across the cerebral cortex, especially in the occipitoparietal regions where alpha rhythms show maximum power. This view assumes that AG plays a role of neural "hub" and propagates the synchronization/desynchronization of low-frequency alpha rhythms across the cerebral cortex. In this framework, alpha power would index the magnitude of cortical inhibition in task-relevant representations, both related to external cognition (e.g., DAN) or internal cognition (e.g., DMN).

A final point of discussion is the right lateralization of the modulation of intrahemispheric coherence, which was stronger for right over left AG. Alpha rhythms are traditionally associated with attention and arousal (Haegens, Luther, & Jensen, 2012; Babiloni et al., 2003). Arousal deficits are classically associated with right hemisphere lesions (Corbetta & Shulman, 2011) including regions of the inferior parietal lobule (supramarginal [SMG] and AG). Although AG is part of the DMN, the SMG along with the TPJ is part of the so-called ventral attention network that is right hemisphere lateralized (Corbetta & Shulman, 2011; Shulman et al., 2010; Liu, Stufflebeam, Sepulcre, Hedden, & Buckner, 2009). These regions have also been implicated in arousal and vigilance (Corbetta & Shulman, 2011). In this study, the right lateralization on alpha coherence may partly reflect a certain suppression of adjacent cortex in SMG.

Conclusions

Inhibitory magnetic stimulation over bilateral AG, one of the core DMN nodes, but not FEF or IPS, core DAN nodes, enhanced resting state, low-frequency alpha power in bilateral occipitoparietal cortex, as well as intrahemispheric alpha coherence (right AG). These results suggest that AG plays a causal role in the modulation and propagation of the resting-state dominant alpha rhythms to the posterior parietal regions.

Acknowledgments

The research leading to these results has received funding from the European Community's Seventh Framework Programme (FP7/2007-2013), Grant Agreement "BrainSynch" HEALTH-F2-2008-200728. M. C. was supported by the National Institute of Mental Health Grants R01 1R01MH096482 and HD061117-05A2 P. C. was supported by a postdoctoral contract from the G. D'Annunzio University Foundation, Chieti, Italy. C. B. was supported by the Italian Ministry of Health Project GR-2008-1143091.

Reprint requests should be sent to Paolo Capotosto, Department of Neuroscience and Imaging, University G. D'Annunzio of Chieti, Istituto di Tecnologie Avanzate Biomediche, Via dei Vestini 33, Chieti, 66100, Italy, or via e-mail: pcapotosto@unich.it.

REFERENCES

Anderson, B., Mishory, A., Nahas, Z., Borckardt, J. J., Yamanaka, K., Rastogi, K., et al. (2006). Tolerability and safety of high daily doses of repetitive transcranial magnetic stimulation in healthy young men. *The Journal of ECT, 22,* 49–53.

Aydin-Abidin, S., Trippe, J., Funke, K., Eysel, U. T., & Benali, A. (2008). High- and low-frequency repetitive transcranial magnetic stimulation differentially activates c-Fos and zif268 protein expression in the rat brain. *Experimental Brain Research, 188,* 249–261. Epub 2008 Apr 2.

Babiloni, C., Brancucci, A., Babiloni, F., Capotosto, P., Carducci, F., Cincotti, F., et al. (2003). Anticipatory cortical responses during the expectancy of a predictable painful stimulation. A high-resolution electroencephalography study. *European Journal of Neuroscience, 18,* 1692–1700.

Babiloni, C., Vecchio, F., Miriello, M., Romani, G. L., & Rossini, P. M. (2006). Visuospatial consciousness and parieto-occipital areas: A high-resolution EEG study. *Cerebral Cortex, 16,* 37–46.

Berger, H. (1929). Über das Elektrenkephalogramm des Menchen. *Archives für Psychiatrie, 87,* 527–570.

Biswal, B., DeYoe, A. E., & Hyde, J. S. (1996). Reduction of physiological fluctuations in fMRI using digital filters. *Magnetic Resonance in Medicine, 35,* 107–113.

Bollimunta, A., Mo, J., Schroeder, C. E., & Ding, M. (2011). Neuronal mechanisms and attentional modulation of corticothalamic α oscillations. *Journal of Neuroscience, 31,* 4935–4943.

Brignani, D., Manganotti, P., Rossini, P. M., & Miniussi, C. (2008). Modulation of cortical oscillatory activity during transcranial magnetic stimulation. *Human Brain Mapping, 29,* 603–612.

Buckner, R. L., Andrews-Hanna, J. R., & Schacter, D. L. (2008). The brain's default network: Anatomy, function, and relevance to disease. *Annals of the New York Academy of Sciences, 1124,* 1–38.

Buckner, R. L., Sepulcre, J., Talukdar, T., Krienen, F. M., Liu, H., Hedden, T., et al. (2009). Cortical hubs revealed by intrinsic functional connectivity: Mapping, assessment of stability, and relation to Alzheimer's disease. *Journal of Neuroscience, 29,* 1860–1873.

Candidi, M., Stienen, B. M., Aglioti, S. M., & de Gelder, B. (2011). Event-related repetitive transcranial magnetic stimulation of posterior superior temporal sulcus improves the detection of threatening postural changes in human bodies. *Journal of Neuroscience, 31,* 17547–17554.

Canolty, R. T., Soltani, M., Dalal, S. S., Edwards, E., Dronkers, N. F., Nagarajan, S. S., et al. (2007). Spatiotemporal dynamics of word processing in the human brain. *Frontiers in Neuroscience, 1,* 185–196. Epub 2007 Oct 15.

Capotosto, P., Babiloni, C., Romani, G. L., & Corbetta, M. (2009). Frontoparietal cortex controls spatial attention through modulation of anticipatory alpha rhythms. *Journal of Neuroscience, 29,* 5863–5872.

Capotosto, P., Babiloni, C., Romani, G. L., & Corbetta, M. (2012). Differential contribution of right and left parietal cortex to the control of spatial attention: A simultaneous EEG-rTMS study. *Cerebral Cortex, 22,* 446–454.

Capotosto, P., Corbetta, M., Romani, G. L., & Babiloni, C. (2012). Electrophysiological correlates of stimulus-driven reorienting deficits after interference with right parietal cortex during a spatial attention task: A TMS-EEG study. *Journal of Cognitive Neuroscience, 24,* 2363–2371.

Chadick, J. Z., & Gazzaley, A. (2011). Differential coupling of visual cortex with default or frontal-parietal network based on goals. *Nature Neuroscience, 14,* 830–832.

Corbetta, M., & Shulman, G. L. (2002). Control of goal-directed and stimulus-driven attention in the brain. *Nature Reviews Neuroscience, 3,* 201–215.

Corbetta, M., & Shulman, G. L. (2011). Spatial neglect and attention networks. *Annual Review of Neuroscience, 34,* 569–599. Review.

Crone, N. E., Sinai, A., & Korzeniewska, A. (2006). High-frequency gamma oscillations and human brain mapping with electrocorticography. *Progress in Brain Research, 159,* 275–295. Review.

Dastjerdi, M., Foster, B. L., Nasrullah, S., Rauschecker, A. M., Dougherty, R. F., Townsend, J. D., et al. (2011). Differential electrophysiological response during rest, self-referential, and non-self-referential tasks in human posteromedial cortex. *Proceedings of the National Academy of Sciences, U.S.A., 108,* 3023–3028. Epub 2011 Jan 31.

de Pasquale, F., Della Penna, S., Snyder, A. Z., Marzetti, L., Pizzella, V., Romani, G. L., et al. (2012). A cortical core for dynamic integration of functional networks in the resting human brain. *Neuron, 74,* 753–764.

Deco, G., & Corbetta, M. (2011). The dynamical balance of the brain at rest. *Neuroscientist, 17,* 107–123. Epub 2010 Dec 31.

Fox, M. D., & Raichle, M. E. (2007). Spontaneous fluctuations in brain activity observed with functional magnetic resonance imaging. *Nature Reviews Neuroscience, 8,* 700–711. Review.

Fox, M. D., Snyder, A. Z., Vincent, J. L., Corbetta, M., Van Essen, D. C., & Raichle, M. E. (2005). The human brain is intrinsically organized into dynamic, anticorrelated functional networks. *Proceedings of the National Academy of Sciences, U.S.A., 102,* 9673–9678.

Freunberger, R., Klimesch, W., Sauseng, P., Griesmayr, B., Höller, Y., Pecherstorfer, T., et al. (2007). Gamma oscillatory activity in a visual discrimination task. *Brain Research Bulletin, 71,* 593–600. Epub 2006 Dec 27.

Fries, P. (2005). A mechanism for cognitive dynamics: Neuronal communication through neuronal coherence. *Trends in Cognitive Sciences, 9,* 474–480.

Friese, U., Supp, G. G., Hipp, J. F., Engel, A. K., & Gruber, T. (2012). Oscillatory MEG gamma band activity dissociates perceptual and conceptual aspects of visual object processing: A combined repetition/conceptual priming study. *Neuroimage, 59,* 861–871. Epub 2011 Jul 30.

Funke, K., & Benali, A. (2010). Cortical cellular actions of transcranial magnetic stimulation. *Restorative Neurology and Neuroscience, 28,* 399–417. Review.

Gonçalves, S. I., de Munck, J. C., Pouwels, P. J., Schoonhoven, R., Kuijer, J. P., Maurits, N. M., et al. (2006). Correlating the alpha rhythm to BOLD using simultaneous EEG/fMRI: Inter-subject variability. *Neuroimage, 30,* 203–213.

Haegens, S., Luther, L., & Jensen, O. (2012). Somatosensory anticipatory alpha activity increases to suppress distracting input. *Journal of Cognitive Neuroscience, 24,* 677–685.

Hagmann, P., Cammoun, L., Gigandet, X., Meuli, R., Honey, C. J., Wedeen, V. J., et al. (2008). Mapping the structural core of human cerebral cortex. *PLoS Biology, 6,* e159.

Harris, I. M., Benito, C. T., Ruzzoli, M., & Miniussi, C. (2008). Effects of right parietal transcranial magnetic stimulation on object identification and orientation judgments. *Journal of Cognitive Neuroscience, 20,* 916–926.

He, B. J., Snyder, A. Z., Vincent, J. L., Epstein, A., Shulman, G. L., & Corbetta, M. (2007). Breakdown of functional connectivity in frontoparietal networks underlies behavioral deficits in spatial neglect. *Neuron, 53,* 905–918.

Klimesch, W., Doppelmayr, M., Russegger, H., Pachinger, T., & Schwaiger, J. (1998). Induced alpha band power changes in the human EEG and attention. *Neuroscience Letters, 244,* 73–76.

Knyazev, G. G., Slobodskoj-Plusnin, J. Y., Bocharov, A. V., & Pylkova, L. V. (2011). The default mode network and EEG α oscillations: An independent component analysis. *Brain Research, 1402,* 67–79. Epub 2011 May 27.

Laufs, K., Krakow, P., Sterzer, E., Eger, A., Beyerle, A., Salek-Haddadi, A., et al. (2003). Electroencephalographic signatures of attentional and cognitive default modes in spontaneous brain activity at rest. *Proceedings of the National Academy of Sciences, U.S.A., 100,* 11053–11058.

Lewis, C. M., Baldassarre, A., Committeri, G., Romani, G. L., & Corbetta, M. (2009). Learning sculpts the spontaneous activity of the resting human brain. *Proceedings of the National Academy of Sciences, U.S.A., 106,* 17558–17563.

Liu, H., Stufflebeam, S. M., Sepulcre, J., Hedden, T., & Buckner, R. L. (2009). Evidence from intrinsic activity that asymmetry of the human brain is controlled by multiple factors. *Proceedings of the National Academy of Sciences, U.S.A., 106,* 20499–20503.

Lorincz, M. L., Kékesi, K. A., Juhász, G., Crunelli, V., & Hughes, S. W. (2009). Temporal framing of thalamic relay-mode firing by phasic inhibition during the alpha rhythm. *Neuron, 63,* 683–696.

Machii, K., Cohen, D., Ramos-Estebanez, C., & Pascual-Leone, A. (2006). Safety of rTMS to non-motor cortical areas in healthy participants and patients. *Clinical Neurophysiology, 117,* 455–471.

Mantini, D., Perrucci, M. G., Del Gratta, C., Romani, G. L., & Corbetta, M. (2007). Electrophysiological signatures of resting state networks in the human brain. *Proceedings of the National Academy of Sciences, U.S.A., 104,* 13170–13175.

Miller, K. J., Weaver, K. E., & Ojemann, J. G. (2009). Direct electrophysiological measurement of human default network areas. *Proceedings of the National Academy of Sciences, U.S.A., 106,* 12174–12177.

Mutanen, T., Mäki, H., & Ilmoniemi, R. J. (2013). The effect of stimulus parameters on TMS-EEG muscle artifacts. *Brain Stimulation, 6,* 371–376.

Pfurtscheller, G., & Andrew, C. (1999). Event-related changes of band power and coherence: Methodology and interpretation. *Journal of Clinical Neurophysiology, 16,* 512–519.

Pfurtscheller, G., & Lopes da Silva, F. H. (1999). Event-related EEG/MEG synchronization and de-synchronization: Basic principles. *Clinical Neurophysiology, 110,* 1842–1857.

Raichle, M. E., MacLeod, A. M., Snyder, A. Z., Powers, W. J., Gusnard, D. A., & Shulman, G. L. (2001). A default mode of brain function. *Proceedings of the National Academy of Sciences, U.S.A., 98,* 676–682.

Rappelsberger, P., & Petsche, H. (1988). Probability mapping: Power and coherence analyses of cognitive processes. *Brain Topography, 1,* 46–54.

Ridding, M. C., & Ziemann, U. (2010). Determinants of the induction of cortical plasticity by non-invasive brain stimulation in healthy subjects. *Journal of Physiology, 588,* 2291–2304. Epub 2010 May 17.

Rossi, S., Hallett, M., Rossini, P. M., & Pascual-Leone, A. (2009). Safety of TMS Consensus Group. Safety, ethical considerations, and application guidelines for the use of transcranial magnetic stimulation in clinical practice and research. *Clinical Neurophysiology, 120,* 2008–2039.

Rossini, P. M., Barker, A. T., Berardelli, A., Caramia, M. D., Caruso, G., Cracco, R. Q., et al. (1994). Non invasive electrical and magnetic stimulation of the brain, spinal cord and roots: Basic principles and procedures for routine clinical application. *Electroencephalography and Clinical Neurophysiology, 91,* 79–92.

Sadaghiani, S., Scheeringa, R., Lehongre, K., Morillon, B., Giraud, A. L., & Kleinschmidt, A. (2010). Intrinsic connectivity networks, alpha oscillations, and tonic alertness: A simultaneous electroencephalography/ functional magnetic resonance imaging study. *Journal of Neuroscience, 30,* 10243–10250.

Sestieri, C., Capotosto, P., Tosoni, A., Romani, G. L., & Corbetta, M. (2013). Interference with episodic memory retrieval following transcranial stimulation of the inferior but not the superior parietal lobule. *Neuropsychologia, 51,* 900–906.

Sestieri, C., Corbetta, M., Romani, G. L., & Shulman, G. L. (2011). Episodic memory retrieval, parietal cortex, and the default mode network: Functional and topographic analyses. *Journal of Neuroscience, 31,* 4407–4420.

Sestieri, C., Shulman, G. L., & Corbetta, M. (2010). Attention to memory and the environment: Functional specialization and dynamic competition in human posterior parietal cortex. *Journal of Neuroscience, 30,* 8445–8456.

Shulman, G. L., Ongür, D., Akbudak, E., Conturo, T. E., Ollinger, J. M., Snyder, A. Z., et al. (1997). Common blood flow changes across visual tasks: II. Decreases in cerebral cortex. *Journal of Cognitive Neuroscience, 9,* 648–663.

Shulman, G. L., Pope, D. L., Astafiev, S. V., McAvoy, M. P., Snyder, A. Z., & Corbetta, M. (2010). Right hemisphere dominance during spatial selective attention and target detection occurs outside the dorsal frontoparietal network. *Journal of Neuroscience, 30,* 3640–3651.

Siegel, M., Donner, T. H., Oostenveld, R., Fries, P., & Engel, A. K. (2008). Neuronal synchronization along the dorsal visual pathway reflects the focus of spatial attention. *Neuron, 60,* 709–719.

Smith, S. M., Fox, P. T., Miller, K. L., Glahn, D. C., Fox, P. M., Mackay, C. E., et al. (2009). Correspondence of the brain's functional architecture during activation and rest. *Proceedings of the National Academy of Sciences, U.S.A., 106,* 13040–13045. Epub 2009 Jul 20.

Steriade, M., Datta, S., Paré, D., Oakson, G., & Curró Dossi, R. C. (1990). Neuronal activities in brain-stem cholinergic nuclei related to tonic activation processes in thalamocortical systems. *Journal of Neuroscience, 10,* 2541–2559.

Thickbroom, G. W. (2007). Transcranial magnetic stimulation and synaptic plasticity: Experimental framework and human models. *Experimental Brain Research, 180,* 583–593. Epub 2007 Jun 12. Review.

Thut, G., Nietzel, A., Brandt, S. A., & Pascual-Leone, A. (2006). Alpha-band electroencephalographic activity over occipital cortex indexes visuospatial attention bias and predicts visual target detection. *Journal of Neuroscience, 26,* 9494–9502.

Trippe, J., Mix, A., Aydin-Abidin, S., Funke, K., & Benali, A. (2009). è Burst and conventional low-frequency rTMS differentially affect GABAergic neurotransmission in the rat cortex. *Experimental Brain Research, 199,* 411–421.

Urgesi, C., Berlucchi, G., & Aglioti, S. M. (2004). Magnetic stimulation of extrastriate body area impairs visual processing of nonfacial body parts. *Current Biology, 14,* 2130–2134.

Urgesi, C., Calvo-Merino, B., Haggard, P., & Aglioti, S. M. (2007). Transcranial magnetic stimulation reveals two cortical pathways for visual body processing. *Journal of Neuroscience, 27,* 8023–8030.

Vaishnavi, S. N., Vlassenko, A. G., Rundle, M. M., Snyder, A. Z., Mintun, M. A., & Raichle, M. E. (2010). Regional aerobic glycolysis in the human brain. *Proceedings of the National Academy of Sciences, U.S.A., 107,* 17757–17762.

Wassermann, E. M. (1998). Risk and safety of repetitive transcranial magnetic stimulation: Report and suggested guidelines from the International Workshop on the Safety of Repetitive Transcranial Magnetic Stimulation, June 5–7, 1996. *Electroencephalography and Clinical Neurophysiology, 108,* 1–16.

Worden, M. S., Foxe, J. J., Wang, N., & Simpson, G. V. (2000). Anticipatory biasing of visuospatial attention indexed by retinotopically specific alpha-band electroencephalography increases over occipital cortex. *Journal of Neuroscience, 20,* RC63.

Wu, L., Eichele, T., & Calhoun, V. D. (2010). Reactivity of hemodynamic responses and functional connectivity to different states of alpha synchrony: A concurrent EEG-fMRI study. *Neuroimage, 52,* 1252–1260.